

Original Article

SYNTHESIS AND EVALUATION OF ZINC SUBSTITUTED MAGNETITE NANOPARTICLES FOR DRUG DELIVERY SYSTEMS

IRYNA VEDERNIKOVA

Department of Inorganic Chemistry, National University of Pharmacy, Pushkinskaya St. 53, 61002 Kharkov, Ukraine
Email: irina.vedernicova@rambler.ru

Received: 09 Jun 2015 Revised and Accepted: 11 Jul 2015

ABSTRACT

Objective: The aim of this study is to synthesis zinc substituted magnetite nanoparticles with higher values of saturation magnetization and testing its antibacterial activity.

Methods: The particles of zinc substituted magnetite with the composition of $Zn_xFe_{3-x}O_4$ ($x = 0.0, 0.2, 0.3, 0.4, 0.5$) were prepared using a chemical condensation method. The crystalline structure, morphology and the magnetic properties of the ferrite particles were studied by means of X-ray diffraction (XRD), transmission electron microscopy (TEM) and vibrating sample magnetometer. The synthesized ZnMNP40 were tested for their antibacterial and antifungal activity by disc diffusion method.

Results: X-ray diffraction analysis showed that the nanoparticles formed in the present synthesis were crystalline (spinel type) in nature. The size of the synthesized nanoparticles was in the range of 3-13 nm obtained from TEM image. Magnetic measurements at 300 K have demonstrated the super paramagnetic behavior of the nanoparticles. The synthesized ZnMNP40 nanoparticles exhibited antibacterial activity against bacterial strains like *Bacillus subtilis*, *Escherichia coli*, *Staphylococcus aureus* and antifungal activity.

Conclusion: Zinc has been incorporated into the crystal structure of magnetite to enhance the saturation magnetization of nanoparticles. The synthesized ZnMNP40 had a nanometric size and a superparamagnetic behavior, exhibited effective antibacterial property.

Keywords: Ferrite nanoparticles, Composition, Structure, Magnetization, Antibacterial activity.

INTRODUCTION

Nanotechnology is one of the most interesting areas of modern science. One of the most promising of nanomaterials is the magnetic nanoparticles (MNPs) of different compositions [1]. MNPs offer exciting opportunities in fundamental studies and technological applications, such as biomedical applications, bio processing and catalysts among many others [2-5]. Due to their unique properties, MNPs have been actively investigated as the component of targeted drug delivery systems [6-8].

Nanoparticles of magnetite are the most widely used sources of magnetic materials. Doping magnetite with transition metal elements (zinc, copper, manganese) allows the modification of important quantities such as saturation magnetization, optical properties, electroconductivity [9-11]. Zinc belongs to a class of microelements that is considered to play an important role in many vital biochemical reactions and physiological processes: growth and development of the cells, stimulation of the gene transcription and cell proliferation, slowing down the oxidation processes, optimization of the human immune system [12-16].

Zinc oxide nanoparticles are used as antimicrobial agent when incorporated into materials such as paints, textiles, plastics and personal care products, and can be added to the food to reduce the food poisoning effect by the various *Aspergillus sp.*, which is legally approved [17-19]. Zinc oxide nanoparticles have shown the best antibacterial behavior compared to copper (II) oxide and iron (III) oxide nanoparticles [20, 21].

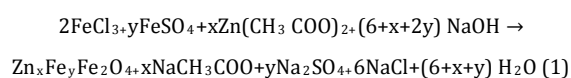
Therefore, to get more information about zinc ferrite nanoparticles ($ZnO \cdot Fe_2O_3$) and to improve their applications or develop new ones, careful studies related to their functionality, particle sizes and also their antimicrobial behavior are essential. In this work, zinc-doped magnetite nanoparticles are synthesized through co-precipitation method. This method may be the most promising one because of its simplicity and productivity. It is widely used for biomedical applications because of the ease of implementation and the need for less hazardous materials and procedures. The crystalline structure of the zinc-doped magnetite nanoparticles was studied by means of X-ray diffraction.

MATERIALS AND METHODS

Synthesis of magnetic nanoparticles

Iron (III) chloride ($FeCl_3 \cdot 6H_2O$) and iron (II) sulfate ($FeSO_4 \cdot 7H_2O$) were purchased from Sinopharm Chemical Reagent Co., Ltd. (Shanghai, China). Zinc acetate $Zn(CH_3COO)_2 \cdot 2H_2O$ and sodium hydroxide (NaOH granules) were purchased from Beijing Chemical Company (Beijing, China). All chemicals with 99.9% of purity, which is used as received without further purification.

Ultrafine particles with the composition of $Zn_xFe_{3-x}O_4$ ($x = 0; 0.2, 0.3, 0.4, 0.5$) were prepared by co-precipitating aqueous solutions of $FeSO_4$, $Zn(CH_3COO)_2$ and $FeCl_3$ mixtures in an alkaline medium with maintaining the appropriate mole ratio according to Eq.(1):



In a typical procedure, 10 % by mass water solution of precursors ($FeSO_4$, $Zn(CH_3COO)_2$ and $FeCl_3$) freshly prepared were mixed together at heating. 0.1 M NaOH solution was added drop-wise with continuous stirring until complete precipitation of the black ferrite was achieved (pH 9–11). The reaction mixtures were maintained at 85-90 °C for 4 h. This time was sufficient for the hydroxides to transform into spinel ferrite. After the system was cooled to room temperature, the precipitates were collected using magnetic separation and washed with distilled water until pH neutral, producing thus samples ZnMNP40.

Characterization

The X-ray diffraction (XRD) patterns of the samples were recorded on a Siemens D500 X-ray powder diffractometer using copper radiation. Slow scans of selected diffraction peaks were carried out in the step mode (step size 0.03 °, measurement time 75 s). The crystallite size of the nanocrystalline samples was measured from the X-ray line broadening using the Debye-Scherrer formula. Magnetization measurements were performed in a vibrating sample

magnetometer at 300 K using a superconducting magnet to produce fields up to 2 kOe. The samples were analyzed in a PEM-125k transmission electron microscope (TEM).

Antimicrobial activity assay

The *in vitro* screening of the antimicrobial activity was carried out by the broth-dilution method using a bacterial suspension of 5×10^5 colony-forming units (CFU)/ml McFarland density. The 24-hour-old bacterial cultures were inoculated into nutrient broth supplemented with various concentrations of ZnMnPs. A control (nutrient broth and culture only) was also prepared. The antimicrobial activities of the as-synthesized nanoparticles were determined against microbial ATCC reference strains. In the present experiment, we used both Gram-positive and Gram-negative bacterial as well as fungal strains.

The microorganisms used for the study were *S. aureus* ATCC 25923, *E. coli* ATCC 25922, *P. aeruginosa* ATCC 27853, *B. subtilis* ATCC 6633, *C. albicans* ATCC 885-653 strains. The suspensions were incubated at 37 °C for 24 h. After incubation, the bacterial growth was visually inspected and the lowest concentration of ZnMnPs at which no observable bacterial growth was taken as the minimum inhibitory concentration (MIC) value. The experiments were carried out in triplicate, and averages were reported. For the determination of the minimum bactericidal concentration (MBC) and minimum fungicidal concentrations (MFC), solid nutrient medium (Mueller-Hinton agar) was inoculated with one loopful of culture taken from the first broth cultures. While MBC assay plates were incubated for at 37 °C for 24 h, MFC assay plates were incubated at 25 °C for 3 days. After incubation, the different levels of the zone of inhibition were measured.

RESULTS AND DISCUSSION

The structural size effect can be revealed in the change of synergy and the constant of the crystalline lattice for finely-dispersed powder without changing crystal symmetry [22, 23]. Therefore, only the change of the lattice constant might be expected. The XRD pattern for zinc-doped magnetite nanoparticles are shown in fig. 1.

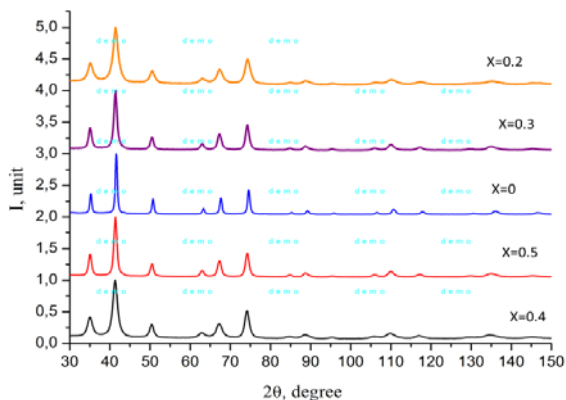


Fig. 1: X-ray diffraction pattern of $Zn_xFe_{3-x}O_4$ composition

The character of diffraction patterns satisfies the powders single phase and indicates the fact that the crystals synthesized have a cubic structure of the spinel type ferrite belonging to $Fd3m(227)$ space group. The crystallite size was estimated by the Debye-Scherrer formula using the full width at half maximum values of the indexed peaks. The average crystallite size decreases from 9.2 to 5.8 nm as the partial substitution of zinc decreases. Although all the samples were prepared under identical conditions, the crystallite size was not the same for all Zn concentrations. This was, probably, due to the preparation conditions, which gave rise to different rates of ferrite formation for different concentrations of zinc, favoring the variation of crystallite size.

The value of the lattice parameters was calculated from diffraction patterns with the error of $(3-4) \cdot 10^{-4} \text{ \AA}$ (fig.2). The lattice constant was found to be increasing with the increase in zinc concentration from $x=0$ to $x=0.4$.

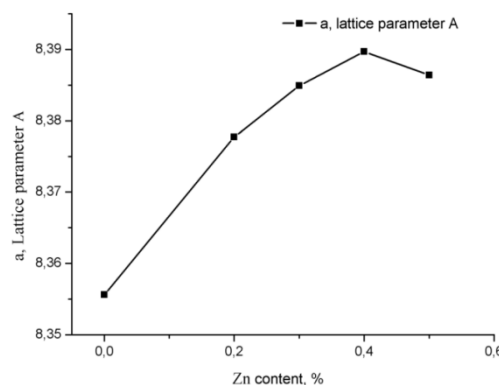


Fig. 2: Dependence of the crystalline lattice of ZnMnPs on the zincions concentration

The lattice constant (*a*) increased with increasing Zn content, which suggested the formation of a compositionally homogeneous solid solution and was found to be within the range of the lattice constants of $FeFe_2O_4$ and $ZnFe_2O_4$. The ionic radii of Zn^{2+} (0.82 Å) and Fe^{2+} (0.83 Å) are almost the same. However, the tetrahedral interstitial site has smaller radii for both Fe_3O_4 (0.55 Å) and $ZnFe_2O_4$ (0.65 Å) than the octahedral interstitial site (0.75 and 0.70 Å, respectively). Thus, the localization of Zn^{2+} ions in the tetrahedral interstitial sites increases the lattice parameter. The observed nonlinear character of dependence $a(x)$ can be due to the fact that the Zn^{2+} ions partially occupy the octahedral positions. In a cubic system of ferromagnetic spinels, the magnetic order is mainly due to a super exchange interaction mechanism occurring between the metal ion in the A and B sublattices. The substitution of nonmagnetic ion such as zinc, which has a preferentially A site occupancy results in the reduction of the exchange interaction between A and B sites. Hence, by varying the amount of zinc substitution, it should be possible to vary magnetic properties of the samples [24]. The saturation magnetization for all the ZnMnPs is listed in table 1.

Table 1: The parameters derived from X-ray diffraction pattern and saturation magnetization of the ZnMnPs

Chemical composition	Mol. mass, (g/mol)	Lattice parameter a (Å)	X-ray density (g/cm ³)	Crystallite size and microstrain, nm/%	Saturation magnetization (emu/g)
$FeFe_2O_4$	232.0	8.3560(3)	5.2854	10.8/0.14	67.4
$Zn_{0.2}Fe_{0.8}Fe_2O_4$	233.8	8.3773(4)	5.2931	7.8/0.60	65.8
$Zn_{0.3}Fe_{0.7}Fe_2O_4$	234.7	8.3841(13)	5.2935	7.0/0.90	54.9
$Zn_{0.4}Fe_{0.6}Fe_2O_4$	235.6	8.3906(3)	5.3054	9.2/0.17	75.2
$Zn_{0.5}Fe_{0.5}Fe_2O_4$	236.5	8.3850(10)	5.3352	5.8/0.50	63.2

The decrease in the particle size to the nanometer scale is accompanied by the decrease in the magnetization all ZnMnPs. The sample ZnMnPs40 has the specific magnetization $M = 75 \text{ emu} \cdot \text{g}^{-1}$ in field $H = 17 \text{ kOe}$ (fig. 3). It is higher than magnetization of magnetite particles ($FeFe_2O_4$) with the same size [25]; i.e., the substitution of zinc ions for iron ions made it possible to increase the magnetization of the nanoparticles. By using the coprecipitation method at room temperature, it is easy to prepare ZnMnPs nanoparticles with an approximate size of 9 nm. The results showed that the crystallite and average particle size of the ZnMnPs were dependent on the concentration of zinc ions.

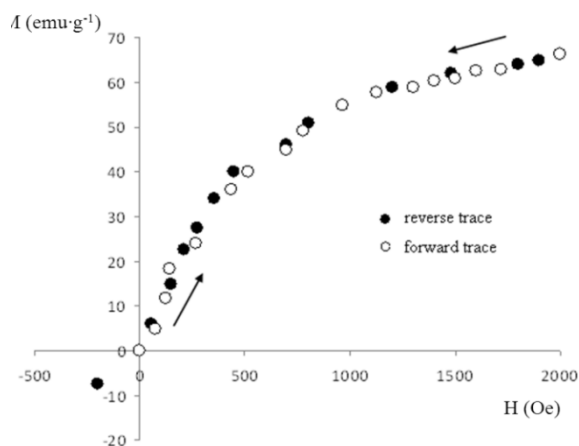


Fig. 3: The fragment of the hysteresis loop of the as-synthesized particles ZnMnPs40

The magnetic measurement confirms that the synthesized particles exhibit superparamagnetic properties at room temperature. The magnetization curve for the ZnMnPs40 exhibits immeasurable values of coercivity field and remnant magnetization (fig.3).

Fig. 4 shows, the TEM image of the particles and their size distribution obtained with a statistic of ~400 particles for the composition with zinc concentration 40 % (ZnMnPs40). The distribution is close to symmetrical, the values of d lie in the range of 3–13 nm, and the average value is ~8.5 nm. In this case, 80% of the particles have the sizes of 6.0–10.0 nm, which agrees with the result obtained by X-ray diffraction.

The antimicrobial activity of the ZnMnPs40 has been studied on strains belonging to common bacterial pathogens, that is, the Gram-negative, *Pseudomonas aeruginosa*, *Escherichia coli*, Gram-positive *Staphylococcus aureus*, *Bacillus subtilis* and fungus. The sample of ZnMnPs40 was found to be active against the test organisms with varying values of MIC (table 2).

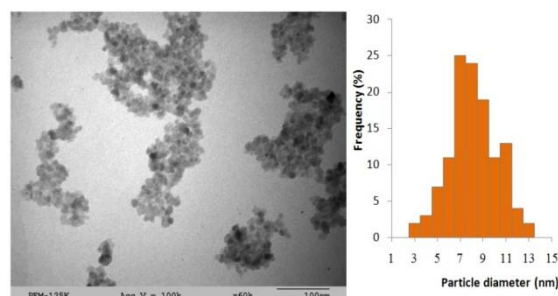


Fig. 4: TEM image and particle size histogram of synthesized nanoparticles ZnMnPs40

The significant inhibitory effect was observed against *Escherichia coli* (gram negative), and *Staphylococcus aureus*, *Bacillus subtilis* (gram positive) bacteria and fungus (table 2). It was found that the ZnMnPs40 exhibited antibacterial activity against *E. coli*, *S. aureus*, *B. subtilis* and antifungal activity with MIC, 62.5 $\mu\text{g/ml}$, and MBC of 125.0 $\mu\text{g/ml}$. The nanoparticles were found to be bacteriostatic and fungistatic in action. Similar activity observations have been made for nanoparticles of zinc oxide [20, 26]. The probable mechanism of the antimicrobial action of ZnMnPs involves the binding of Zn^{2+} ions to the functional groups of proteins and enzymes, which causes inactivation and inhibition in cell processes. Zinc ions cause destruction of the bacterial cell wall, degradation and lysis of the cytoplasm; leading to cell death. ZnMnPs with the size 9 nm have a large surface area, thus their bactericidal efficacy is enhanced compared to largersized particles. For the zinc nanoparticles system, studies [26-28] showed that zinc binds to the membranes of microorganisms, similar to mammalian cells, prolonging the lag phase of the growth cycle and increasing the generation time of the organisms so that it takes each organism more time to complete cell division.

Zinc oxide nanoparticles potentiate bactericidal efficacy of macrolides, tetracyclines and beta lactum antibiotics [29]. Future studies should investigate the effect of ZnMnPs on the antibacterial activity of different antibiotics and the applicability of these nanoparticles for magnetic targeted drug delivery system will also be investigated.

Table 2: Antimicrobial activity of ZnMnPs40 nanoparticle

Pathogen	Concentration ($\mu\text{g/ml}$)	Observation	MIC ($\mu\text{g/ml}$)	Zone of inhibition (mm) \pm SD (n=3)	MBC/MFC ($\mu\text{g/ml}$)
<i>Staphylococcus aureus</i> (ATCC 25923)	control	turbid	-	-	-
	15.6	turbid	-	-	-
	31.2	turbid	-	-	-
	62.5	clear	62.5	-	-
	125.0	clear	-	9.5 \pm 0.1	125.0
	250.0	clear	-	11.2 \pm 0.1	-
<i>Bacillus subtilis</i> (ATCC 6633)	control	turbid	-	-	-
	15.6	turbid	-	-	-
	31.2	turbid	-	-	-
	62.5	clear	62.5	-	-
	125.0	clear	-	7.6 \pm 1.0	125.0
	250.0	clear	-	9.0 \pm 0.5	-
<i>Escherichia coli</i> (ATCC 25922)	control	turbid	-	-	-
	15.6	turbid	-	-	-
	31.2	turbid	-	-	-
	62.5	clear	62.5	-	-
	125.0	clear	-	12.1 \pm 0.2	125.0
	250.0	clear	-	14.0 \pm 1.0	-
<i>Pseudomonas aeruginosa</i> (ATCC 27853)	control	turbid	-	-	-
	15.6	turbid	-	-	-
	31.2	turbid	-	-	-
	62.5	turbid	-	-	-
	125.0	turbid	-	-	-
	250.0	clear	250.0	-	-
	500.0	clear	-	8.6 \pm 0.8	500.0

	control	turbid	-	
	15.6	turbid	-	
<i>Candida albicans</i>	31.2	turbid	-	
(ATCC 885-653)	62.5	clear	62.5	-
	125.0	clear		11.0±0.7
	250.0	clear		13.4±1.0
	500.0	clear		17.5±0.3
				125.0

CONCLUSION

Co-precipitation method has been used to synthesize the magnetite system with the composition of $Zn_xFe_{3-x}O_4$ ($x=0-0.5$). The lattice constant and particle size were found to be increasing with the increase in zinc concentration from $x=0$ to $x=0.4$. The resulting ZnMnPs exhibit superparamagnetic properties, depending on the particle size: the lower the particle size, the lower is the saturation magnetization. The synthesized ZnMnPs40 being combinations of superparamagnetic behavior, higher value of saturation magnetization with small particle size, appear to be of interest for biomedical applications. It was found that the ZnMnPs40 exhibited antibacterial activity against *E. coli*, *S. aureus*, *B. subtilis* and antifungal activity. The prepared ZnMnPs40 can be used for further studies and applications as drug delivery systems.

ACKNOWLEDGEMENT

The author would like to acknowledge Dr. V. V. Kazmirchuk head of Antibacterial Agents Laboratory, Mechnicov Institute of Microbiology and Immunology for assistance with antimicrobial investigation and to the staff of the Physics Faculty of V. N. Karazin Kharkiv National University for their help with this research.

CONFLICT OF INTERESTS

Declared None

REFERENCES

- Mudshinge SR, Deore AB, Patil S, Bhargat CM. Nanoparticles: emerging carriers for drug delivery. Saudi Pharm J 2011;19:129-41.
- Krishnan K. Biomedical nanomagnetism: a spin through possibilities in imaging, diagnostics, and therapy. IEEE Trans Magn 2010;46:2523-58.
- Tartaj P, Morales M, Veintemillas-Verdaguer S, Gonz'alez T, Serna C. The preparation of magnetic nanoparticles for applications in biomedicine. J Phys D: Appl Phys 2003;36:182-97.
- Faraji M, Yamini Y, Rezaee M. Magnetic nanoparticles: synthesis, stabilization, functionalization, characterization, and applications. J Iran Chem Soc 2010;7:1-37.
- Indira TK, Lakshmi MK. Magnetic nanoparticles—a review. Int J Pharm Sci Nanotechnol 2010;3:1035-42.
- Sangeetha N, Kumaraguru AK. Antitumor effects and characterization of biosynthesized iron oxide nanoparticles using seaweeds of Gulf of Mannar. Int J Pharm Pharm Sci 2015;7:469-76.
- Koppiseti V, Sahiti B. Magnetically modulated drug delivery systems. Int J Drug Dev Res 2011;3:260-6.
- Saiyed Z, Telang S, Ramchand C. Application of magnetic techniques in the fields of drug discovery and biomedicine. BioMagnetic Res Technol 2003;1:1-13.
- Girgis E, Wahsh M, Othman A, Bandhu L, Rao KV. Synthesis, magnetic and optical properties of core/shell $Co_{1-x}Zn_xFe_2O_4/SiO_2$ nanoparticles. Nanoscale Res Lett 2011;6:1-12.
- Kharkwal R, Uma S, Nagarajan R. Synthesis and optical properties of pure $CdTiO_3$ and Ni^{2+} and Zn^{2+} ion substituted $CdTiO_3$ obtained by a novel precursor route. Indian J Chem 2012;51A:1538-44.
- Krishna RK, Ravinder D, Kumar K. Thermo electrical power studies of nickel-zinc ferrites synthesized by citrate gel technique. Int J Eng Res Ind Appl 2013;3:1459-68.
- Chu A, Foster M, Hancock D, Bell-Anderson K, Petocz P, Samman S. TNF- α gene expression is increased following zinc supplementation in type 2 diabetes mellitus. Genes Nutr 2015;10:1-10.
- Miceli MV, Tatejr DJ, Alcock NW, Newsome DA. Zinc deficiency and oxidative stress in the retina of pigmented rats. Invest Ophthalmol Visual Sci 1999;40:1238-44.
- Harr'us U, Baumeister P, Zieger S, Matthias C. The influence of high doses of vitamin C and zinc on oxidative DNA damage. Anticancer Res 2005;25:3197-202.
- Osredkar J, Sustar N. Copper and zinc, biological role and significance of copper/zinc imbalance. J Clin Toxicol 2011;3:2-18.
- Prasad AS. Zinc: role in immunity, oxidative stress and chronic inflammation. Curr Opin Clin Nutr Metab Care 2010;12:646-52.
- Baskar G, Chandhuru J, Fahad S, Praveen A. Mycological synthesis, characterization and antifungal activity of zinc oxide nanoparticles. Asian J Pharm Technol 2013;3:142-6.
- Xie Y, He Y, Irwin P, Jin T, Shi X. Antibacterial activity and mechanism of action of zinc oxide nanoparticles against *Campylobacter jejuni*. Appl Environ Microbiol 2011;77:2325-31.
- Zhang LL, Jiang YH, Ding YL, Povey M, York D. Investigation into the antibacterial behaviour of suspensions of ZnO nanoparticles (ZnO nanofluids). J Nanopart Res 2007;9:479-89.
- Azam A, Ahmed A, Oves M, Khan M, Habib S, Memic A. Antimicrobial activity of metal oxide nanoparticles against Gram-positive and Gram-negative bacteria: a comparative study. Int J Nanomed 2012;7:6003-9.
- Gordon T, Perlstein B, Houbara O, Felner I, Banin E, Margel S. Synthesis and characterization of zinc/iron oxide composite nanoparticles and their antibacterial properties. Colloids Surf A 2001;374:1-8.
- Mathew DS, Juang RS. An overview of the structure and magnetism of spinel ferrite nanoparticles and their synthesis in microemulsions. Chem Eng J 2007;129:51-65.
- Kumar L, Kumar P, Narayan A, Kar M. Rietveld analysis of XRD patterns of different sizes of nanocrystalline cobalt ferrite. Int Nano Lett 2013;3:26-34.
- Singhal S, Namgyal T, Bansal S, Chandra K. Effect of Zn substitution on the magnetic properties of cobalt ferrite nanoparticles prepared via sol-gel route. J Electromagn Anal Appl 2010;2:376-81.
- Mahdavi M, Ahmad MB, Haron M, Namvar F, Nadi B, Zaki M, et al. Synthesis, surface modification and characterisation of biocompatible magnetic iron oxide nanoparticles for biomedical applications. Molecules 2013;18:7533-48.
- Navale GR, Thripuranthaka M, Late DJ, Shinde SS. Antimicrobial activity of ZnO nanoparticles against pathogenic bacteria and fungi. J Sci Med Nanotechnol Nanomed 2015;3:2-9.
- Atmaca S, Gul K, Cicek R. The effect of zinc on microbial growth. Turk J Med Sci 1998;28:595-7.
- Goudouri O, Kontonasaki E, Lohbauer U, Boccaccini A. Antibacterial properties of metal and metalloid ions in chronic periodontitis and peri-implantitis therapy. Acta Biomater 2014;10:3795-810.
- Chandrika R, Mayi P, Kumar R. Role of ZnO nanoparticles in enhancing the antibacterial activity of antibiotics. Asian J Pharm Clin Res 2012;5:97-9.